

# 論文内容の要旨

## The dynamic changes in the structures and electronic states of supported metal catalysts in redox processes characterized by time-resolved x-ray absorption fine structure (XAFS)

時間分解 XAFS による金属担持触媒活性中心の酸化還元反応に伴う構造及び電子状態変化の動的機構の解明  
氏名：上村洋平

### Introduction

A goal of catalytic chemistry is to understand key issues to control dynamic catalysis of nanoparticles and surfaces by *in situ* characterization techniques, because new catalysts in industry have been developed in try-and-error type investigation, and rational design of nanoparticle catalysts and surfaces is still hard to achieve in a molecular level. Among many characterization techniques, x-ray absorption fine structure (XAFS) is one of the most powerful techniques for characterization of structures and electronic states of supported metal catalysts which have been employed in a variety of industrial chemical processes as well as in sustainable green processes, environmentally benign processes, automobile exhaust cleaning processes, fuel cells. Recently, time-resolved Dispersive-XAFS(DXAFS) has received much attention as an inevitable technique to discover the origin and mechanism of the genesis of efficient solid catalysis.

In this study, I have explored dynamic changes in the structure and electronic state of supported metal catalysts in redox processes by *in situ* time-resolved DXAFS, choosing two types of supported metal catalysts, a Re<sub>10</sub> cluster catalyst supported on HZSM-5 zeolite(Re/HZSM-5) for catalytic phenol synthesis from benzene and O<sub>2</sub> and two kinds of PtSn bimetallic nanoparticle catalysts supported on  $\gamma$ -Al<sub>2</sub>O<sub>3</sub> for reforming process and on active carbon for fuel cell.

### Experimental

**Sample preparation** ; A 0.6 wt% Re/HZSM-5 catalyst was prepared by Chemical Vapor Deposition of CH<sub>3</sub>ReO<sub>3</sub>. A  $\gamma$ -Al<sub>2</sub>O<sub>3</sub>-supported Pt-Sn catalyst was prepared by a conventional impregnation method using 0.4 M HCl aq. A carbon (KETJEN BLACK ECP600JD)-supported Pt-Sn catalyst was also prepared by a conventional adsorption method as follows; typically 0.14 g H<sub>2</sub>PtCl<sub>6</sub>·6H<sub>2</sub>O was dissolved into 0.1 M HCl aq. or 1 M HCl aq., and 0.061 g SnCl<sub>2</sub>·2H<sub>2</sub>O was added to each solvent under continuously stirring. The solution was stirred for 5 h at R.T. and then filtered. The remaining powder was kept under vacuum over night. The samples prepared with 1 M HCl aq. and 0.1 M HCl aq. are denoted as 1 M PtSn/C and 0.1 M PtSn/C, respectively.

**In situ XAFS measurement** ; All *in situ* XAFS measurements were conducted at the Photon Factory in KEK. *In situ* DXAFS experiments at Re L<sub>III</sub>-edge were performed by a Bragg-type curved Si(111) crystal polychromator ( $R = 2.5$  m) and a photo-diode array equipped with a phosphorescent device. *In situ* step-scan and quick XAFS measurements at Pt L<sub>III</sub> edge were mainly carried out at the beamline of 9A, 9C, and 12C with Si(111) double crystal monochromators (DCM), and some XAFS measurements at Pt-L<sub>III</sub> edge and all *in situ* XAFS measurements at Sn K-edge were conducted at the beamline of NW10A with Si(311) DCM. *In situ* DXAFS measurements at Pt L<sub>III</sub>-edge and Sn K-edge were measured at the beamline of NW2A. A Bragg-type Si(311) curved crystal polychromator( $R = 1.5$  m) was used for Pt L<sub>III</sub>-edge measurements and a Laue-type Si(511) curved crystal polychromator( $R = 0.9$  m) was used for Sn K-edge measurements.

## Results and Discussions

### The oxidation of active $\text{Re}_{10}$ clusters supported on HZSM-5

Phenol is one of the most important industrial chemicals, but its chemical process, called as cumene process, has some drawbacks such as low-one path efficiency or treatments of lots of by-products. The direct phenol synthesis by the selective oxidation of benzene with molecular oxygen has been the most desired process and explored for decades in the light of economy and environment. The  $\text{Re}_{10}$  cluster supported on HZSM-5 is the first promising catalyst which transforms benzene to phenol with 93.9% selectivity at 9.9% conversion.

Fig. 1(a) shows  $\text{Re L}_{\text{III}}$ -edge time-resolved XAFS spectra for the  $\text{Re}_{10}$  cluster/HZSM-5 catalyst under  $\text{O}_2$  atmosphere at 553 K, where the active  $\text{Re}_{10}$  cluster transforms to the inert  $\text{ReO}_4$  monomer. In the time-resolved XAFS spectra, there were observed three isosbestic points. It indicates that the XAFS spectra can be described as  $\mu t(E, t) = c(t)\mu t(E, 0) + (1 - c(t))\mu t(E, \infty)$ ;  $\mu t(E, 0)$  is the initial spectrum and  $\mu t(E, \infty)$  is the final spectrum. The coefficient  $c(t)$  was described as  $c(t) = Ae^{-k't}$  from the fitting results, where  $k'$  is the apparent rate constant. This implies that the oxidation of the  $\text{Re}_{10}$  cluster on HZSM-5 is

of the first order to  $[\text{Re}_{10}]$ . Thus, it is suggested that a  $\text{Re}_{10}$  cluster is swiftly oxidized to  $\text{ReO}_4$  monomers without formation of any undesirable intermediates and this should be a key of the high selectivity of the  $\text{Re}/\text{HZSM-5}$  catalyst. *In situ* DXAFS measurements were conducted under  $\text{O}_2$  and  $\text{Bz} + \text{O}_2$  atmosphere at several temperature. The similar analysis of these results gives Fig. 1(b) shows the Arrhenius plots of the oxidation of  $\text{Re}_{10}$  species under  $\text{O}_2$  and  $\text{Bz} + \text{O}_2$ . Their activation energies ( $E_a$ ) were calculated to be  $49 \text{ kJ mol}^{-1}$  and  $74 \text{ kJ mol}^{-1}$ , respectively. Although the reaction steps under the both atmospheres are the same, the activation energy was different from each other. Benzene shows a positive effect on stabilizing the active cluster structure under the reaction atmosphere and this is a key of its high catalytic performance.

### The reaction mechanism of phase separation of the Pt-Sn nanoparticles

Supported Pt-Sn bimetal catalysts are used as a multifunctional catalyst for reforming, alkane dehydrogenation, fuel cell electrode. Pt-Sn bimetal catalysts are also tolerant to CO poisoning, which is especially beneficial for commercial fuel cell electrodes. Although the Pt-Sn bimetal catalysts have advantages in catalytic properties and economical efficiency, the bimetal phase can be dephased with dissociation of nano-alloy phase by oxidation, and this is supposed to induce leaching of the Pt and Sn ions on the electrode and decrease the catalytic activity. The information on the dynamic formation and dissociation of nano-alloy particles is crucial to understand and improve the leaching processes.

#### The kinetic analysis of the oxidation of $\text{PtSn}/\gamma\text{-Al}_2\text{O}_3$

From XRD pattern and *in situ* EXAFS experiments, the Pt-Sn alloy was formed on  $\gamma\text{-Al}_2\text{O}_3$  after reduction and it was mainly the  $\text{Pt}_3\text{Sn}_1$  structure, which has the fcc structure and longer lattice constants than Pt bulk. Pt and Sn have been oxidized in 30 min under  $\text{O}_2$  atmosphere at 673 K. Fig. 2(a) shows the results of *in situ* DXAFS measurements

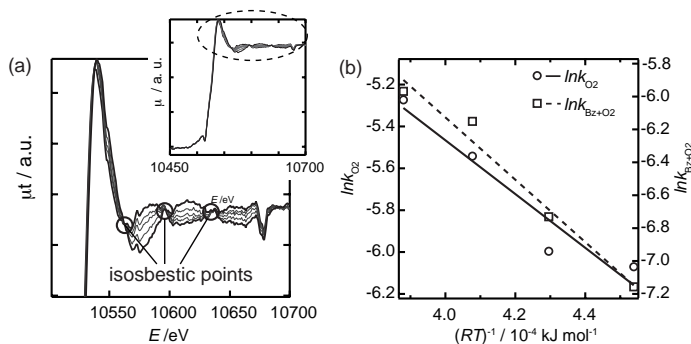


Fig. 1 (a) Time-resolved XAFS spectra of  $\text{Re L}_{\text{III}}$ -edge under  $\text{O}_2$  atmosphere, where the spectrum was measured in 0.1 s every 1 s. (b) Arrhenius plots of the oxidation of the  $\text{Re}_{10}$  clusters under  $\text{O}_2$  and a mixture of benzene and  $\text{O}_2$ .

at Pt L<sub>III</sub>-edge for PtSn/γ-Al<sub>2</sub>O<sub>3</sub>.

The  $\mu t(E_1, t)$  of Pt L<sub>III</sub>-edge was fitted well with the double exponential function as  $\mu t(E_1, t) = c_1 e^{-k_1' t} + c_2 e^{-k_2' t}$ . This indicates that the oxidation of Pt in PtSn/γ-Al<sub>2</sub>O<sub>3</sub> proceeds through at least two successive reactions. Fig. 2(c) shows the change of the white line intensity of Pt L<sub>III</sub>-edge at different  $P_{O_2}$ . The kinetic analyses were performed in the following manner; the white line intensity,  $\mu t(E_1, t)$ , was plotted against the reaction time( $t$ ) in Fig. 2 (b) and the function  $\mu t(E_1, t)$  was fitted by  $\mu t(E_1, t) = \sum c_i e^{-k_i' t} + y_0$  with the minimum i. Here  $k_i'$  is an apparent rate constant, which depends on the pressure of gaseous oxygen. Supposing O<sub>2</sub> adsorbs molecularly, the number of O<sub>2</sub>(ad) is described as  $NKP_{O_2}(1 + KP_{O_2})^{-1}$ , thus  $k_i'$  is described as  $k_i' = k_i(T)NKP_{O_2}(1 + KP_{O_2})^{-1}$ .  $N$  is the number of adsorption point on the surface of nanoparticle and  $K$  is adsorption equilibrium constant for O<sub>2</sub> and  $k_i$  is a true rate constant. The  $k_i'$  plot against  $P_{O_2}$  was fitted with the function to extract  $k_i(T)$ .

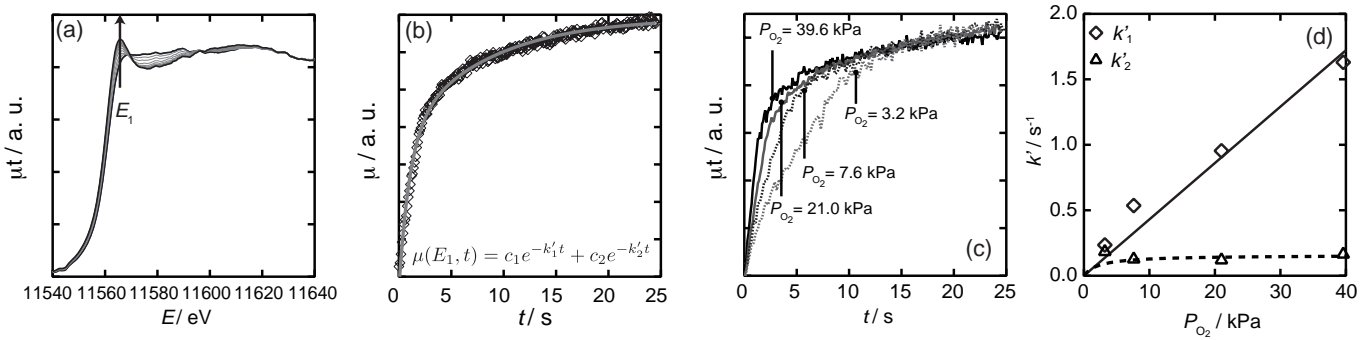


Fig. 2 (a) The time-resolved XAFS spectra of PtSn/γ-Al<sub>2</sub>O<sub>3</sub> Pt L<sub>III</sub> edge in the oxidation process at  $P_{O_2} = 21.0$  kPa and  $T = 673$  K. (b) the change in the intensity of the white line of (a). (c) the variation of the intensity of white line under several  $P_{O_2}$ . (d) the rate constants for the oxidation of PtSn/γ-Al<sub>2</sub>O<sub>3</sub>.

Each line has a turnoff point (pointed in Fig. 2(c)). It takes longer time for  $\mu t(E_1, t)$  to reach the point as  $P_{O_2}$  becomes lower. Fig. 2(d) shows the dependence of  $k'$  for the oxidation of Pt on  $P_{O_2}$ . As the  $k_1'$  is proportional to  $P_{O_2}$ ,  $KP_{O_2}$  must be much smaller than 1 and the number of O<sub>2</sub> adsorbed on the surface of the nanoparticles is much lower than that at saturation. Thus  $k'$  can be described as  $k' = kNKP_{O_2}$ . On the other hand,  $k_2'$  is independent of  $P_{O_2}$ . This means the equilibrium constant  $K$  is much larger than that of the first oxidation process.

Fig. 3(a) shows the change of the white line intensity,  $\mu t(E_1, t)$ , at Sn K-edge for PtSn/γ-Al<sub>2</sub>O<sub>3</sub>. The intensity of the white line of Sn K-edge is described by a single step scheme  $c \cdot e^{-k' t}$  in contrast to the oxidation of Pt. And the apparent rate constant of the oxidation of  $P_{O_2}$  (Fig. 3 (b)). These facts indicate that Pt and Sn can be oxidized simultaneously at the beginning of the oxidation process. Although Sn is oxidized through single process, Pt is not completely oxidized in the first step. Sn is comparable to that of the first oxidation step of Pt and the dependence of  $k'$  is also in proportion to  $P_{O_2}$ .

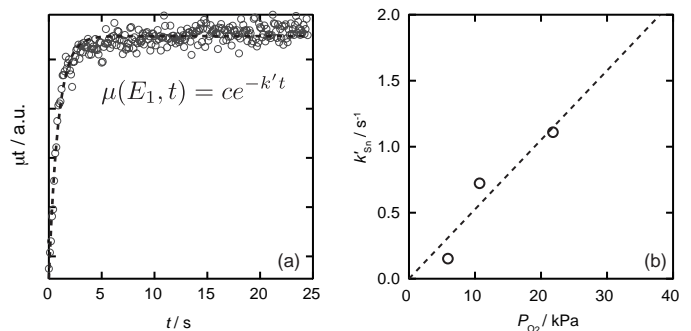


Fig. 3(a) The change of the white line intensity at Sn K-edge at  $P_{O_2} = 23.6$  kPa and  $T = 673$  K. (b) the rate constants for the oxidation of Sn in PtSn/γ-Al<sub>2</sub>O<sub>3</sub>.

It is supposed that Pt nanoparticles are constructed after the first oxidation step and it is gradually oxidized. High-resolution TEM images for Pt/SnO<sub>2</sub> showed formation of Pt nanoparticles surrounded by amorphous SnO<sub>x</sub> on SnO<sub>2</sub>

under the similar oxidation condition to the present XAFS experiment. The whole oxidation process of PtSn/ $\gamma$ -Al<sub>2</sub>O<sub>3</sub> may be described as follows; Pt and Sn in the PtSn/ $\gamma$ -Al<sub>2</sub>O<sub>3</sub> are oxidized simultaneously at the beginning, which is the phase separation process, and Pt becomes nanoparticles surrounded by amorphous SnO<sub>x</sub>.

*The kinetic analysis of the oxidation of 1 M PtSn/C(Pt<sub>3</sub>Sn<sub>1</sub>/C) and 0.1 M PtSn/C(Pt<sub>1</sub>Sn<sub>1</sub>/C)*

The PtSn structure in the reduced 1M PtSn/C and the reduced 0.1 M PtSn/C were Pt<sub>3</sub>Sn<sub>1</sub> and Pt<sub>1</sub>Sn<sub>1</sub> determined by XRD and EXAFS, respectively. PtSn alloy has several kinds of structure according to the atomic ratio of Sn and Pt. Especially the Pt<sub>3</sub>Sn<sub>1</sub> structure is considered as the active structure of the electrode of fuel cell. Here the structure of PtSn alloy is formed selectively with changing the concentration of HCl. Fig. 4(a) shows the results of *in situ* DXAFS experiments at Pt-L<sub>III</sub> edge for 1M PtSn/C, whose main structure is Pt<sub>3</sub>Sn<sub>1</sub>. The change of the intensity of white line is analyzed under the assumption of the single step scheme. Fig. 4 (b) shows the plot of  $k'$  against  $P_{O_2}$ , where  $k'$  is described as  $kNK P_{O_2} / (1 + K P_{O_2})$  and  $k = 1.3 \text{ s}^{-1}$  and  $K = 0.044$ . *In situ* DXAFS measurements at Sn K-edge for Pt<sub>3</sub>Sn<sub>1</sub>/C were also conducted. The oxidation process of Sn was also fitted by a single exponential curve, resulted in  $k = 1.3 \text{ s}^{-1}$ .

By examining the change of white line intensity over longer time, it was obtained that Sn was completely oxidized in 10 s and that Pt was gradually oxidized over 600 s like the oxidation of PtSn/ $\gamma$ -Al<sub>2</sub>O<sub>3</sub>. This indicates that Pt is not oxidized in the single process. This is because SnO<sub>x</sub> covers Pt after the first oxidation step like the case of PtSn/ $\gamma$ -Al<sub>2</sub>O<sub>3</sub>.

*In situ* Pt L<sub>III</sub>-edge DXAFS spectra of 0.1 M PtSn/C, whose main structure is Pt<sub>1</sub>Sn<sub>1</sub>, are shown in Fig. 5(a). The change of white line intensity is described as the single step scheme, but Pt of Pt<sub>1</sub>Sn<sub>1</sub>/C is less oxidized than that of Pt<sub>3</sub>Sn<sub>1</sub>/C. The pressure dependence of  $k'$  is indicated in Fig. 5(b).  $k$  was calculated as  $0.75 \text{ s}^{-1}$  from the plot of  $k'$  against  $P_{O_2}$ . The rate constant of the Pt oxidation in Pt<sub>1</sub>Sn<sub>1</sub>/C is smaller than that of Pt<sub>3</sub>Sn<sub>1</sub>/C. But, the rate constant of the Sn oxidation was comparable to that for Pt<sub>3</sub>Sn<sub>1</sub>/C. Sn of the Pt<sub>1</sub>Sn<sub>1</sub>/C was completely oxidized. Considering the results of high-resolution TEM of Pt/SnO<sub>2</sub>, SnO<sub>x</sub> is produced in the oxidation of Pt<sub>1</sub>Sn<sub>1</sub>/C and the Pt nanoparticles in Pt<sub>1</sub>Sn<sub>1</sub>/C. Thus the Pt nanoparticle is kept away from the gas phase O<sub>2</sub> due to the SnO<sub>x</sub> coverage. The oxidation of Pt nanoparticle in PtSn/C is strongly affected by the content of Sn in the initial PtSn bimetal nanoparticles. The *in situ* DXAFS revealed the kinetic parameters and dynamic oxidation behaviors for each of Pt and Sn sites in the Pt-Sn bimetal nanoparticles supported on active carbon.

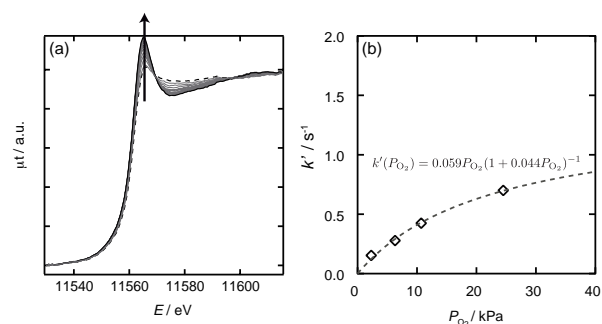


Fig. 4 (a) The Pt L<sub>III</sub>-edge time-resolved XAFS spectra of Pt<sub>3</sub>Sn/C at  $p_{O_2} = 20 \text{ kPa}$  and  $T = 573 \text{ K}$ . (b) the rate constants for the oxidation of Pt<sub>3</sub>Sn/C.

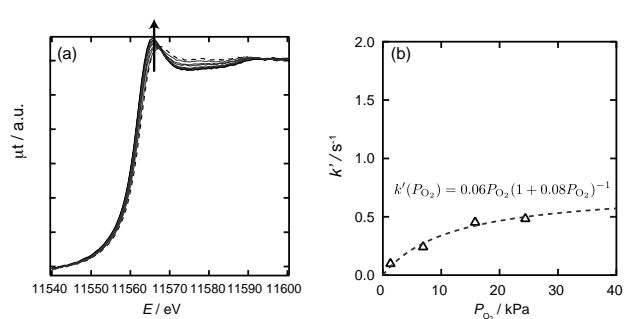


Fig. 5 (a) The Pt L<sub>III</sub>-edge time-resolved XAFS spectra of PtSn/C at  $PO_2 = 20 \text{ kPa}$  and  $T = 573 \text{ K}$ . (b) the rate constants of oxidation of PtSn/C.